ROCK MASS CHARACTERIZATION OF PRIMARY COPPER ORE FOR CAVING AT THE EL TENIENTE MINE, CHILE

By Andres Brzovic[1] and Ernesto Villaescusa, Ph.D.[2]

ABSTRACT

Rock masses of the primary copper ore at the El Teniente Mine are very competent and massive. The rock mass contains almost no open discontinuities. Nevertheless, there is a high frequency network of small discontinuities coupled with widely spaced faults. A data collection campaign designed to characterize the rock structure was recently implemented. The results show that conventional analysis in terms of discontinuity frequency does not predict differences between two studied sectors. However, when an empirical definition of a weak discontinuity is applied, appreciable differences between the two sectors appear in terms of discontinuity frequency and predicted in situ block size distributions. These differences are in accordance with actual observations at the mine site. Due to the geological features of the primary copper ore, rock mass classification schemes cannot be readily applied to characterize these rock masses.

INTRODUCTION

Rock mass classification systems have been developed and used since the 1950s as useful design tools in civil and mining projects. Initially developed for tunneling reinforcement [Terzaghi 1946], these have been extended to multiple civil engineering applications [Barton et al. 1974; Hoek et al. 1995; Laubscher 1993].

The rock mass classification schemes are based on the parameterization of the geological features of the rock mass. These systems simplify the rock mass into two main components: the intact rock properties and the discontinuity characteristics. The International Society for Rock Mechanics (ISRM) has suggested guidelines to characterize these geological features [ISRM 1978].

Following ISRM's guidelines, a data collection campaign designed to characterize the rock structure of the primary copper ore was implemented recently at the El Teniente Mine. This paper presents some results of this current research [Brzovic 2005]. Some data analyses previously published [Brzovic et al. 2006; Brzovic and Villaescusa 2007] are used here since they are relevant to consider when the rock mass classification schemes are applied.

El Teniente Mine Overview

The El Teniente Mine, located in the Andes Mountains in central Chile, 70 km south of Santiago (Figure 1), is one of the largest underground mine operations in the world. Since 1906, more than 1.1 billion tons of ore has been mined. The mine is a stated-owned company (Codelco), and it is currently extracting 131,000 tons per day using block-caving methods. Panel (called conventional) and pre-undercut caving methods [Rojas et al. 2000b], variations of standard block caving, were introduced in 1982 and 1994, respectively, to exploit the primary copper ore (Figure 2).
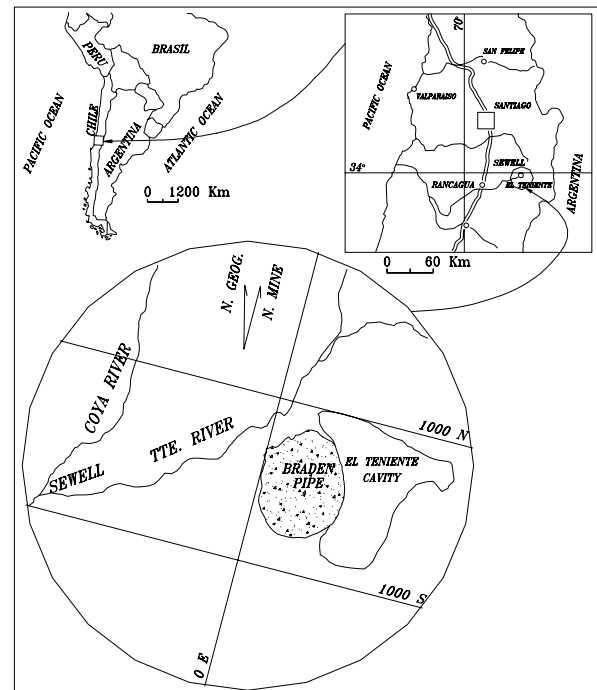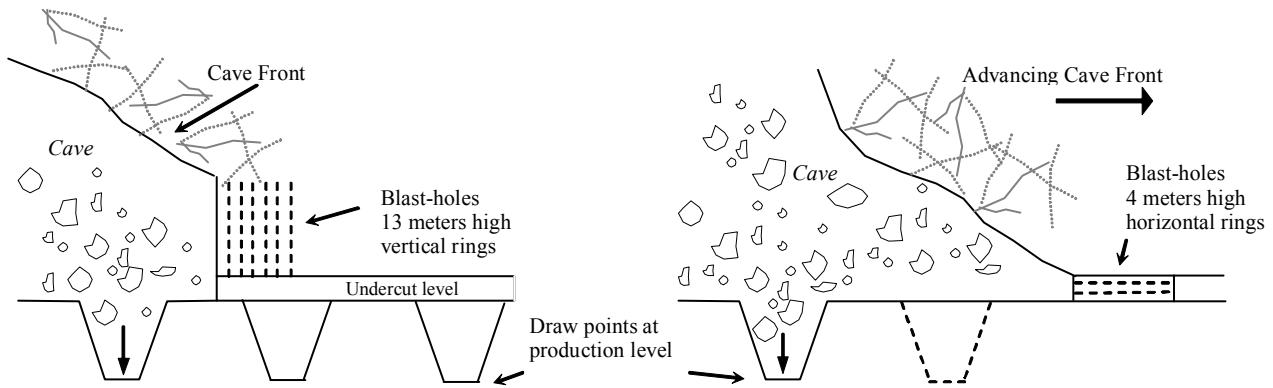

Figure 1.—Location of the El Teniente Mine.

[1]CRC Mining, Western Australian School of Mines, Kalgoorlie, Australia, and Codelco Division El Teniente, Millan, Rancagua, Chile.
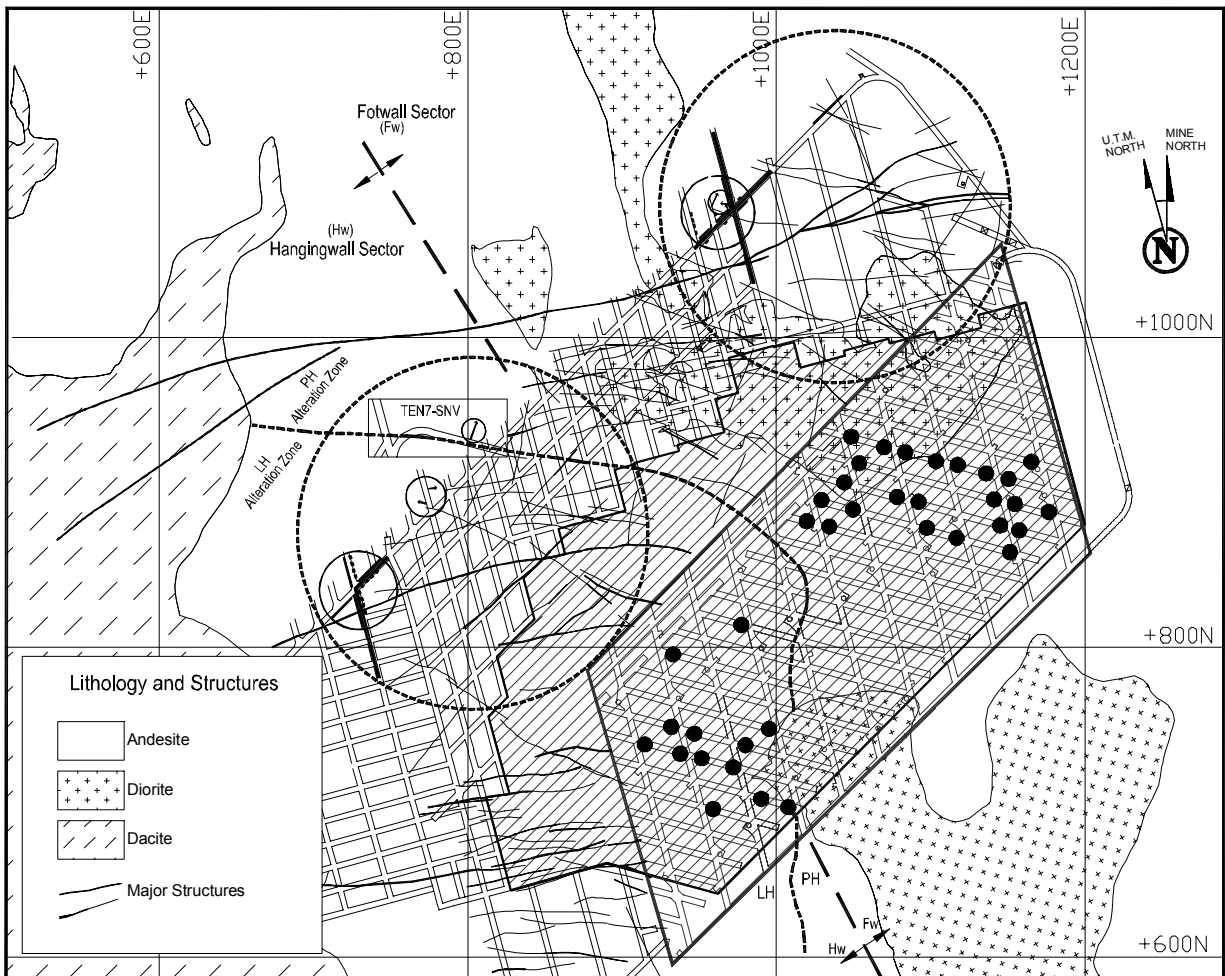[2]CRC Mining, Western Australian School of Mines, Kalgoorlie, Australia.

Conventional panel caving cross section

Pre-undercutting caving cross section

Figure 2.—Panel and pre-undercut caving methods at the El Teniente Mine.
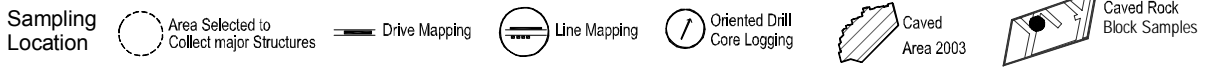

Undercut level of the Teniente Sub-6 mine sector

Figure 3.—Geology of the studied sectors and sampling locations for line sampling techniques and the collected caved rock blocks.
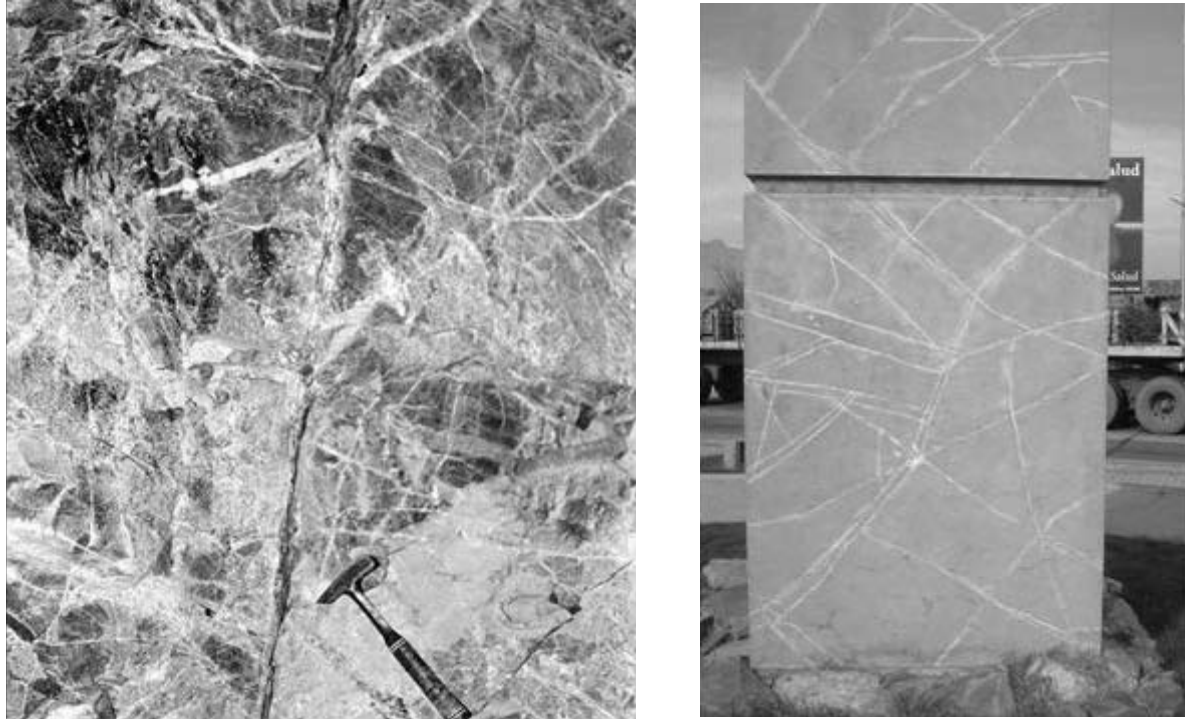
Figure 4.—Stockwork veins (most white lines) and faults (middle of the left photo) recognized within the primary copper ore. The right photo is rock block (1.4-m-long base) showing the stockwork veins, which is used as a monument in Rancagua, Chile.

Currently, almost all of the caving operations are being undertaken within primary copper ore. Such rock masses are very competent and massive, exhibiting brittle, often violent failure under high-stress conditions [Rojas et al. 2000a]. Caving generally results in large rock fragments. Despite these unfavorable rock mass conditions, high rates of production have been achieved since primary copper ore extraction by the conventional panel caving method began in 1982.

Geology and Rock Mass Properties

El Teniente is the largest known copper-molybdenum deposit in the world [Skewes et al. 2006]. It is hosted in a copper porphyry system [Cannell et al. 2005]. The main rock types include a mafic intrusive complex (andesite for this paper), felsic porphyry intrusive (dacite and diorite) and hydrothermal breccias (Braden breccia) of the Miocene Era (Figure 3). Two main structure types are observed within the primary copper ore: a system of large-scale faults [Garrido et al. 1994] and a stockwork having a high frequency of small-scale vein features [Brzovic and Villaescusa 2007; Cuadra 1986], as shown in Figure 4.

The stockwork veins observed within primary copper ore are mainly filled and cemented (healed) with quartz, sulfides, and anhydrite (Figure 4). Different vein types have been identified, and these define alteration zones according to their local abundance. Main alteration zones

are referred to as shown in Figure 3: the late hydrothermal (LH) zone and the principal hydrothermal (PH) zone [Cuadra 1986].

Open joints are rarely found within the primary copper ore, and faults have a very low frequency of occurrence in line sampling (0.1 m^{-1}) [Brzovic 2001]. Joints and faults are the only open discontinuities at the El Teniente Mine. Thus, the primary copper ore rock mass prior to caving can be described as very competent, massive, and impermeable. Intact rock mass properties and rating of rock mass quality used in current mine planning, for main rock types, are presented in Table 1 [Celhay et al. 2005].

Data Collection Design

In order to characterize the rock structure of the primary copper ore, line sampling techniques were undertaken in mine drives within two levels of the Teniente Sub-6 Mine sector (Figure 3). Two structural domains referred to as andesite Hw (hangingwall) and Fw (footwall) were characterized by applying different truncation and censoring biases [Brady and Brown 2003; Villaescusa 1990]. These sampling biases can be considered as different mapping scales (Table 2). A detailed description of the sampling regime adopted in this study is presented by Brzovic and Villaescusa [2007].

Table 1.—Mean of the intact rock mass properties and rock mass quality used for main rock types [Celhay et al. 2005]

Rock type	Intact rock properties				Rock mass rating		
	Density (ton/m³)	E (GPa)	ν	UCS (MPa)	RMR_L	Q′	GSI
Braden breccias....................	2.61	21	0.19	70	—	—	—
Dacite	2.63	30	0.18	90	59–66	22–32	75–95
Diorite	2.77	45	0.21	140	64	19	75–90
Andesite...............................	2.77	56	0.20	115	53–59	19–22	70–85

NOTE.—E, Young's modulus; ν, Poisson's ratio; RMR_L from Laubscher [1993]; Q′ adapted from Barton et al. [1974]; and Geological Strength Index (GSI) from Hoek et al. [1995].

Table 2.—Censoring level, truncation biases, and sample length applied to different line sampling techniques

Sampling method	Censoring level[1] (m)	Truncation bias (m)	Range of the horizontal sample length (m)
Major structure interpretation........	—	30	150
Drive mapping	4.4–4.9	4	30–150
Line mapping	3.6–4	[2]0.3	7–22
Oriented drill core logging.............	0.1–0.14	[2]0.1	4–12

[1]Censoring level only considers the maximum high or width of the observation window.
[2]Some discontinuities longer than the threshold value could not be collected during data collection.

ROCK STRUCTURE CHARACTERIZATION

Although 8 of the 10 suggested parameters by ISRM were fully characterized in both sectors [Brzovic 2005], only the relevant ones are detailed in the following sections.

Discontinuity Occurrence at Different Mapping Scales

Taking into account the main geological discontinuities found within primary copper ore [Brzovic 2001; Cuadra 1986; Garrido et al. 1994], the occurrence for main discontinuity types observed in line mapping is presented in Table 3.

Although the occurrence of discontinuities does not consider the natural anisotropy of the rock structure, some relevant aspects are deduced from Table 3. This is considering the fact that, in most cases, a similar sampling orientation with respect to discontinuity orientation was used for all of the mapping scales [Brzovic and Villaescusa 2007]. Firstly, excluding faults, open joints are not found within the primary copper ore; instead, a large number of veins were recognized (Figure 4). Secondly, faults were better characterized using large-scale sampling. In contrast, veins were better characterized using small-scale sampling. In other words, faults and veins are present within the primary copper ore at different scales. These discontinuity characteristics do not depend on the sampling regime, as discussed by Brzovic and Villaescusa [2007].

Table 3.—Discontinuity type occurrence observed for each data collection technique

Sampling method	Sector	Data	Discontinuity occurrence (%)	
			Faults	Veins
Major structures interpretation...........	Hw	21	57.1	42.9
	Fw	22	77.3	22.7
Drive mapping	Hw	239	16.7	83.3
	Fw	206	30.5	69.5
Lines mapping	Hw	521	1.9	98.1
	Fw	319	7.2	92.8
Oriented drill core logging....................	Hw	606	0.3	99.7
	Fw	565	1.9	98.1

Hw Hangingwall.   Fw Footwall.

Discontinuity Orientation

Faults were found defining one or two subvertical sets at each sector (using large mapping scale). Although subhorizontal faults were not entirely defined by large-scale sampling, the fault data are in agreement with the strike-slip fault characteristics described at the mine scale [Garrido et al. 1994]. In contrast, data from small-scale sampling show that, for both sectors, the veins comprise at least three semiorthogonal discontinuity sets. Figure 5 shows examples of both fault and vein contour orientations from drive and line mapping at the Hw sector.
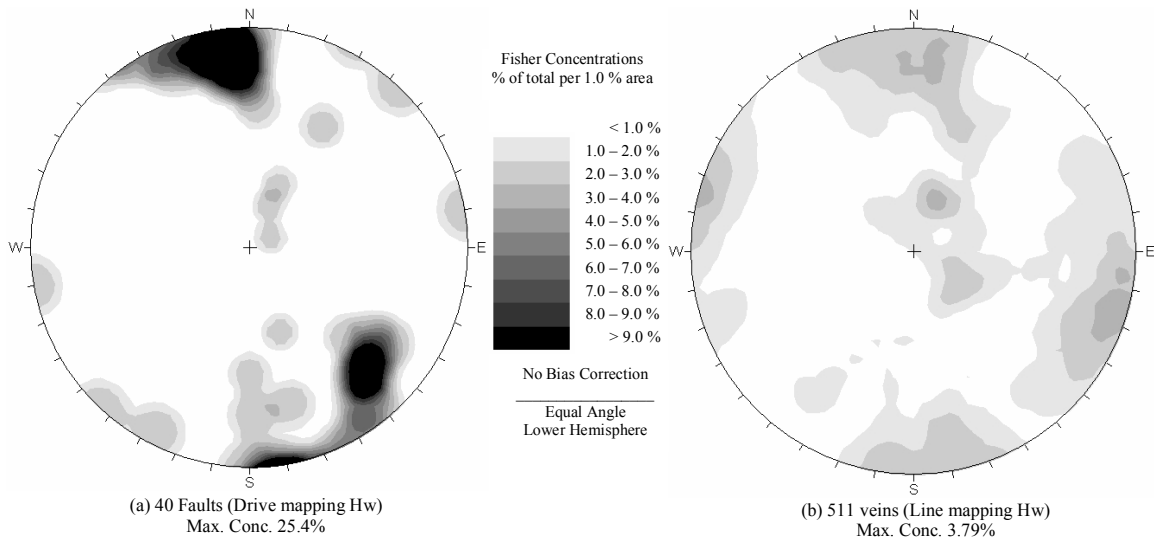
(a) 40 Faults (Drive mapping Hw)
Max. Conc. 25.4%

(b) 511 veins (Line mapping Hw)
Max. Conc. 3.79%

Figure 5.—Fault (a) and vein (b) contour orientations plotted in lower hemisphere projections.

Discontinuity Spacing

The mean normal fault set spacing determined only by large-scale sampling ranges mainly between 5 and 10 m, which is in agreement with previous work [Brooks et al. 1996; Brzovic 2001]. Conversely, high vein frequency was found using small-scale sampling. However, the discontinuity spacing is strongly influenced by the truncation bias used, as Figure 6 shows. Assuming that each truncation level applied represents a mapping scale, the mean normal discontinuity set frequency may be represented as a fractal feature within the rock mass. Scaling law properties (fractal and lineal) for the spacing on other parameters of the geological discontinuities have been proposed by several authors [Cladouhos and Marrett 1996; Gillespie et al. 1993; Hobbs 1993; Scholz 2002], which are consistent with this finding. It is important to recognize that the truncation bias used during data collection plays a relevant role in the spacing obtained, particularly if the rock mass classification schemes are applied.
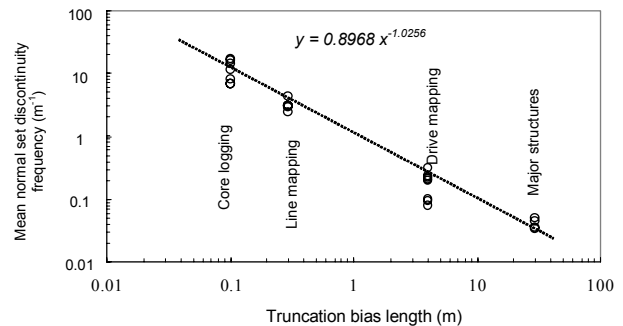

$$y = 0.8968\,x^{-1.0256}$$

Figure 6.—Discontinuity frequency and truncation bias length.

Table 4.—Extremes in values of discontinuity frequency and their orientation using three-dimensional loci [Hudson and Priest 1983]

Sampling method	Global type	Andesite Hw		Andesite Fw	
		Discontinuity frequency (m^{-1})	Trend/Plunge	Discontinuity frequency (m^{-1})	Trend/Plunge
Line mapping	Maxima	6.53	062/48	8.82	064/34
	Minima	2.34	197/07	2.23	257/68
	Mean	4.97		5.74	
	Coefficient of variation	17%		25%	
Oriented drill core logging	Maxima	29.70	036/17	28.56	342/02
	Minima	8.69	280/05	4.61	225/65
	Mean	19.32		16.90	
	Coefficient of variation	26%		32%	

Hw Hangingwall.   Fw Footwall.

Additionally, using the proposed discontinuity frequency diagram, three-dimensional loci [Hudson and Priest 1983], the global maxima and minima, and their orientations for discontinuity frequencies were estimated for both sectors (Table 4). This table also includes the mean discontinuity frequency as the average values obtained from more than 8,000 equidistant directions. This mean value would represent the discontinuity frequency normalized with respect to the orientation at this location.

Table 4 confirms the strong influence of the truncation bias in the discontinuity frequency gathered from a rock mass. It also shows that, in terms of structural anisotropy, both sectors are quite similar when considering the same mapping scale, but minor differences appear when comparing the same sectors at different mapping scales. Therefore, the data in Table 4 show negligible differences between the andesite sectors when all discontinuity types are considered.

Vein Infill

The infill observed in veins was studied by a quantitative estimation of their mineral composition. For instance, a vein could be described as containing 25% quartz, 50% chalcopyrite, and 25% anhydrite. This quantitative infill description was only undertaken at small sampling scales, i.e., line mapping and oriented drill core logging.

The results show that more than nine mineral species were present within the vein infill. Rarely was one mineral present in all veins, and rarely did this mineral maintain the same proportion of abundance as infill throughout all veins (Tables 5–6). In fact, some particular mineral compositions and associated alteration halos have been used to classify vein types at the El Teniente ore deposit [Cuadra 1986]. Nevertheless, four main mineral species were found to be the most common and abundant in all veins recognized during this study: chlorite, anhydrite, chalcopyrite, and quartz (Table 6).

In addition, in terms of veins infill, no substantial differences could be observed between discontinuity sets from the same mapping scale/sector. For example, Table 7 presents discrete data for the sets observed in Figure 5b. In this table, a similar infill pattern is observed for each set. The individual values are similar to the mean of the sector. However, the mineralogical composition was found to have some particular differences between andesite sectors.

Table 5.—Mean of mineral species observed as vein infill, by data collection technique and sector

Sampling method	Sector	Data	Mean of mineral specie observed as vein infill (%)						
			Chlorite	Biotite	Anhydrite	Chalcopyrite	Pyrite	Quartz	Other
Line mapping	Hw	511	6.8	1.7	17.4	13.0	0.2	56.5	4.4
	Fw	296	10.0	1.6	21.7	29.7	2.8	31.5	2.7
Drill core logging	Hw	604	5.5	5.0	2.6	13.0	0.3	68.9	4.7
	Fw	554	13.2	3.7	16.5	26.8	3.9	32.4	3.5

Table 6.—Percentage of mineral species observed as infill within all veins, by data collection technique and sector

Sampling method	Sector	Data	Proportion of veins having the mineral specie as infill (%)						
			Molybdenite	Chlorite	Biotite	Anhydrite	Chalcopyrite	Pyrite	Quartz
Line mapping	Hw	511	6.5	52.8	12.3	71.2	80.2	3.1	91.8
	Fw	296	6.4	58.4	12.8	84.8	94.6	17.9	86.8
Drill core logging	Hw	604	5.6	38.1	22.5	18.7	80.0	2.5	94.9
	Fw	554	3.1	67.5	25.4	70.6	96.6	31.9	86.3

Table 7.—Mean of mineral species observed as vein infill for each family set (refer to Figure 5b) using line mapping at Hw sector

Sampling method	Data	Mean of mineral specie observed as vein infill (%)						
		Chlorite	Biotite	Anhydrite	Chalcopyrite	Pyrite	Quartz	Other
Random	30	5.2	2.3	16.7	8.2	0.6	61.5	5.5
Set 1 (subvertical E–W)	173	6.1	1.5	17.0	13.6	0.2	55.8	5.8
Set 2 (subvertical N–S)	142	8.8	2.5	23.9	13.1	0.4	48.3	3.0
Set 3 (subhorizontal)	166	6.2	1.0	12.4	13.2	0.2	63.3	3.7
Total and mean	511	6.8	1.7	17.4	13.0	0.2	56.5	4.4

Table 8.—Vein thickness distribution for each family set observed (refer to Figure 5b) using line mapping at Hw sector

Family set	Data	Thickness distribution observed (%)					
		<1 mm	1 to <2 mm	2 to <3 mm	3 to <5 mm	5 to <10 mm	≥10 mm
Random	30	16.7	56.7	10.0	6.7	3.3	6.7
Set 1 (subvertical E–W)	172	13.4	40.1	19.8	18.6	7.0	1.2
Set 2 (subvertical N–S)	139	10.1	61.9	10.1	8.6	5.8	3.6
Set 3 (subhorizontal)	165	12.7	45.5	15.2	12.7	6.1	7.9
Total and mean	506	12.5	48.8	15.0	13.2	6.1	4.3

Table 9.—Vein thickness distribution occurrence observed in veins for each data collection technique

Sampling method	Truncation bias length	Data	Thickness distribution observed (%)					
			<1 mm	1 to <2 mm	2 to <3 mm	3 to <5 mm	5 to <10 mm	≥10 mm
Drive mapping	4 m	342	—	5.5	11.7	41.9	25.4	15.5
Line mapping	0.3 m	802	13.3	48.9	15.8	14.9	4.2	2.9
Drill core logging (φ = 10–14 mm)	0.1 m	1126	26.3	44.2	13.6	11.7	2.6	1.6
Drill core logging (φ = 4.6 mm)	[1]0.03 m	Many[2]	64.0	21.5	7.7	4.3	1.8	0.7

[1]Although there was not a truncation bias length threshold criterion during drill core logging, the practical length threshold is esti-mated at around 0.03 m based on the ability to visually identify discontinuity during core logging.
[2]Mean obtained from 108 core section samples 6.1 m long collected from multiple directions [Brzovic 2005].

Vein Thickness

Data analysis of the vein thickness distribution also showed that no differences between discontinuity sets from the same mapping scale at any sector could be observed. Similar to the vein infill, Table 8 shows almost the same vein thickness distribution for each set of data plotted in Figure 5b. The vein set thickness distribution is the same as the mean of the sector.

Nevertheless, similar to discontinuity spacing, Table 9 suggests that the distribution of vein thicknesses observed in line sampling was strongly affected by the truncation level applied. Additional (thinner) discontinuities appeared as the truncation length value was decreased. In this table, data collected by standard unoriented drill core (46-mm-diam) are included [Brzovic 2005] and confirm this finding. This vein characteristic is in agreement with the linear relationship observed between vein length and aperture in several different geological environments [Vermilye and Scholz 1995].

Therefore, two important facts can be deduced. Firstly, assuming a representative sample size, the observed vein thickness distributions (and also the vein infill pattern) can be considered to have an isotropic characteristic within the rock mass, i.e., a linear sampling scheme will define the same thickness distributions at any discontinuity orientation. Secondly, longer discontinuities recognized at the El Teniente Mine tend to be statistically thicker than shorter ones. Furthermore, data analysis indicated that the vein infill does not show changes as the vein thickness varies (Figure 7).
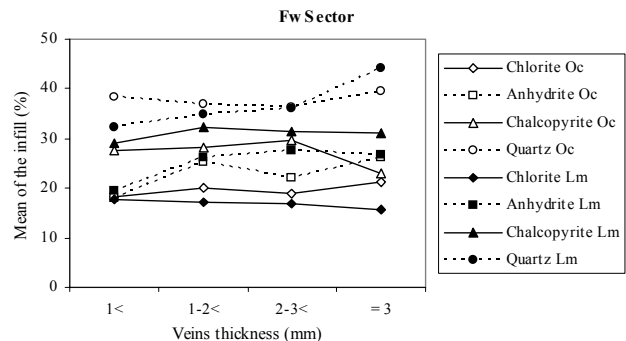

Figure 7.—Relationship between thicknesses and the mean of the mineralogical infill in veins observed at the Fw sector. (Oc = oriented drill core; Lm = line mapping.)

In Situ Rock Block Size Distribution

In order to obtain the in situ rock block distribution and for illustrative purposes only, the data gathered from oriented drill core logging were simulated using a software program [Thompson 2002]. This program assumes a Fisher distribution for orientation, negative exponential distribution for spacing, and infinite trace length for discontinuities (Figure 8). Similar to the discontinuity frequency, Figure 8 shows that the in situ rock block size distributions are practically the same between the andesite sectors.
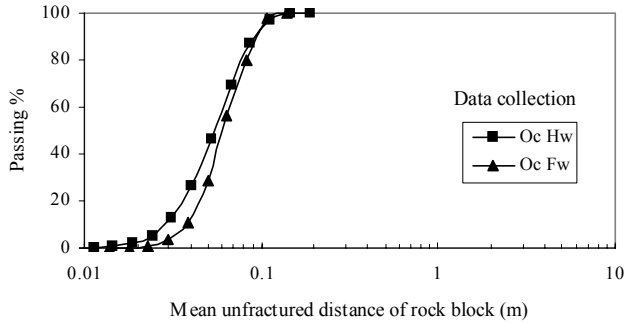
Figure 8.—In situ block size distributions from rock structure simulation. (Oc = oriented drill core.)

WEAK DISCONTINUITIES AT THE EL TENIENTE MINE

The data analysis presented so far included all discontinuities recognized within the rock mass of primary copper ore. However, it is not expected that veins having intermediate- or high-tensile strength (veins having abundant quartz as infill) would be dominant during rock mass disassembly by caving.

Laubscher and Jakubec [2000] have incorporated the effect of healed veins in their proposed methodology to estimate the quality of a jointed rock mass. They described veins as cemented filled joints. However, because of the lack of data regarding the mechanical properties of veins, they proposed the use of the Mohs scale of hardness [Laubscher and Jakubec 2000] to define their frictional properties. In this proposed methodology, veins filled with quartz are ignored due to their strong strength. However, this work does not specify how to proceed when a vein is filled with more than one mineral having different hardnesses, as is the case for most discontinuities recognized at the El Teniente Mine (Tables 5–7).

The lack of experimental determination of the vein infill strength [Willoner 2000] led the authors to study the characteristics of caved rock blocks at the draw points. The objective was to find a common mineralogical association ensemble in veins that defined caved rock block faces during the rock mass disassembly by caving.

This study was carried out at the production level of the Teniente Sub-6 Mine sector (Figure 3), and its major finding was explained in detail by Brzovic et al. [2006] and Brzovic and Villaescusa [2007]. The main conclusion reached was an empirical definition of weak discontinuities, which are those veins having less than 35% of hard minerals as infill. A hard mineral was particularly defined as having a Mohs scale of hardness greater than 4 [Hurlbut 1941]. This finding was gathered from the commonly observed characteristics in 639 veins forming caved rock block faces (Figure 9). These veins were significant weaknesses within the rock mass during the caving and subsequent fragmentation process.

The following comparisons of the El Teniente rock structure are made, taking into account the overwhelming effect of weak discontinuities.

ROCK STRUCTURE CHARACTERIZATION USING ONLY WEAK DISCONTINUITIES

The cumulative frequency of veins collected using oriented drill core logging in terms of their abundance of hard minerals as infill is shown in Figure 10. This figure shows that for the threshold value adopted here (veins filled up to 35% of hard infill), the weak discontinuities represent 16.3% and 49.9% of all discontinuities observed in andesite Hw and andesite Fw, respectively. Figure 10 also shows that appreciable differences between these sectors still appear if a different threshold value of hard infill would be adopted.
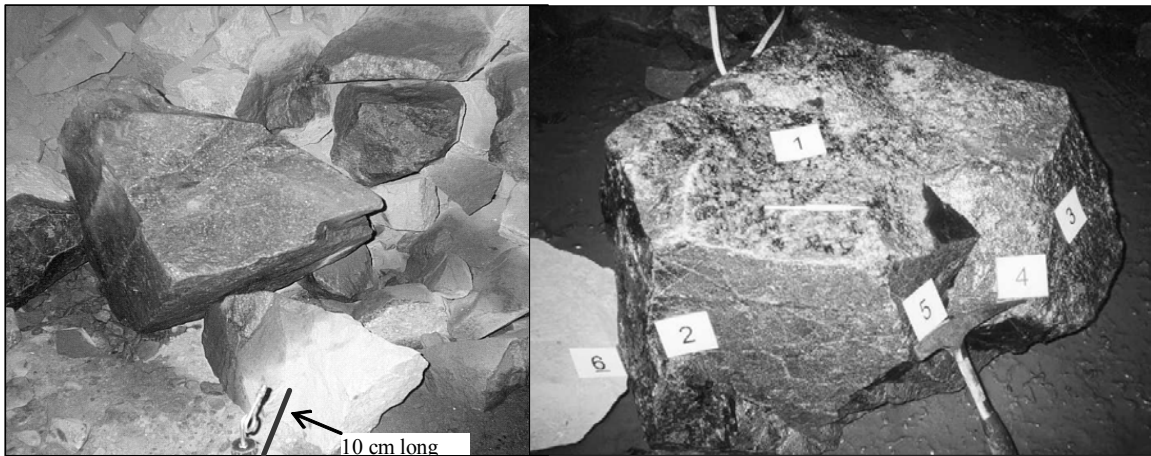

Figure 9.—Veins as faces of polyhedral caved rock blocks in draw points showing mineralogical infill such as chalcopyrite and quartz.
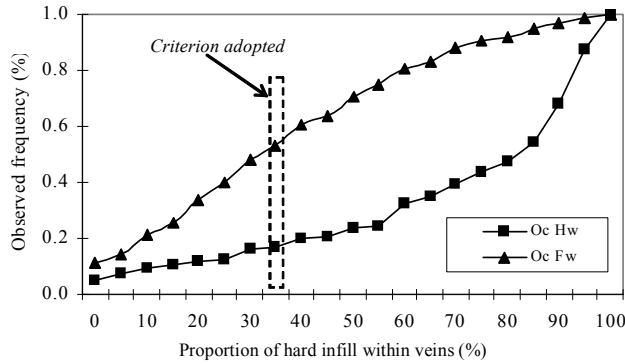
Figure 10.—Cumulative frequency of veins collected using oriented drill core logging (Oc) in terms of the hard minerals as infill. Dashed line shows the criterion of weak discontinuities used in this study.

Figure 11.—Ratio between weak and all discontinuities.

Weak Discontinuity Spacing

Since weak discontinuities are a subgroup of all discontinuities, the mean normal weak discontinuity set spacing was estimated using the same set definition. Using the three-dimensional loci [Hudson and Priest 1983], the global maxima and minima and their orientations for weak discontinuity frequencies were estimated for both sectors (Table 10). No appreciable differences in structural anisotropy can be determined when only the weak discontinuities are considered and compared to when all discontinuities are considered. This can be concluded by comparing Tables 4 and 10. These conclusions reveal two important things. First, they confirm the isotropic characteristic of the vein infill within the rock mass. Second, the different thickness distributions observed at both mapping scales do not affect the vein infill characteristics, as suggested by Figure 7.

Table 10 clearly shows that at any mapping scale the andesite rock type from the Fw sector has a larger frequency of weak discontinuities. According to drill core data, the normalized frequency of weak discontinuities within the Fw sector is nearly three times that of the Hw sector.

In addition, using only data collected by oriented drill core and line mapping from both sectors, the ratio between weak discontinuities and all discontinuities per each discontinuity set is calculated and presented in Figure 11. The data shown in this figure suggest that weak discontinuities are homogeneously distributed within any discontinuity set.

Weak Discontinuity Persistence

The discontinuity trace length features were only studied using line mapping at mine drives. Data analysis of the weak discontinuity trace length distribution showed that no differences between discontinuity sets could be observed (Table 11). This finding is consistent with a circular shape of discontinuities, which always present the same distribution pattern at any rock exposure [Warburton 1980]. Then, the mean value of the trace length distribution for the whole sector can be calculated. Table 11 also shows that the trace length distribution of any set of the Hw sector (plotted in Figure 5b) is almost the same as the mean of the sector. Moreover, Figure 12 reveals that the mean trace length distribution of each sector for weak and all discontinuities are practically the same.

Table 10.—Extremes in values of discontinuity frequency and their orientation of weak discontinuities using three-dimensional loci [Hudson and Priest 1983]

Sampling method	Global type	Andesite Hw		Andesite Fw	
		Discontinuity frequency (m^{-1})	Trend/Plunge	Discontinuity frequency (m^{-1})	Trend/Plunge
Line mapping	Maxima	3.29	066/47	4.88	062/36
	Minima	0.80	197/07	1.41	257/68
	Mean	2.44		3.24	
	Coefficient of variation	23%		24%	
Oriented drill core logging	Maxima	5.62	027/06	15.40	340/00
	Minima	1.04	280/05	2.88	225/65
	Mean	3.46		9.11	
	Coefficient of variation	35%		31%	

**Table 11.—Weak discontinuity trace length distribution for each family set observed (refer to Figure 5b)
using line mapping at Hw sector**

Family set	Data	Trace length distribution observed (%)						
		<0.5 m	0.5 to <1.0 m	1.0 to <1.5 m	1.5 to <2.0 m	2.5 to <3.0 m	3.0 to <4.0 m	≥4 m
Set 1 (subvertical E–W)	52	3.8	23.1	15.4	11.5	21.2	11.5	13.5
Set 2 (subvertical N–S)	44	4.5	15.9	29.5	18.2	11.4	9.1	11.4
Set 3 (subhorizontal)	34	5.9	8.8	14.7	17.6	11.8	11.8	29.4
Total and mean of Hw sector	134	4.5	17.2	20.1	15.7	15.7	10.4	16.4

NOTE.—Data collection by line mapping used a threshold value of 0.3 m as truncation bias.

**Table 12.—Weak discontinuity thickness distribution for each family set observed (refer to Figure 5b)
using line mapping at Hw sector**

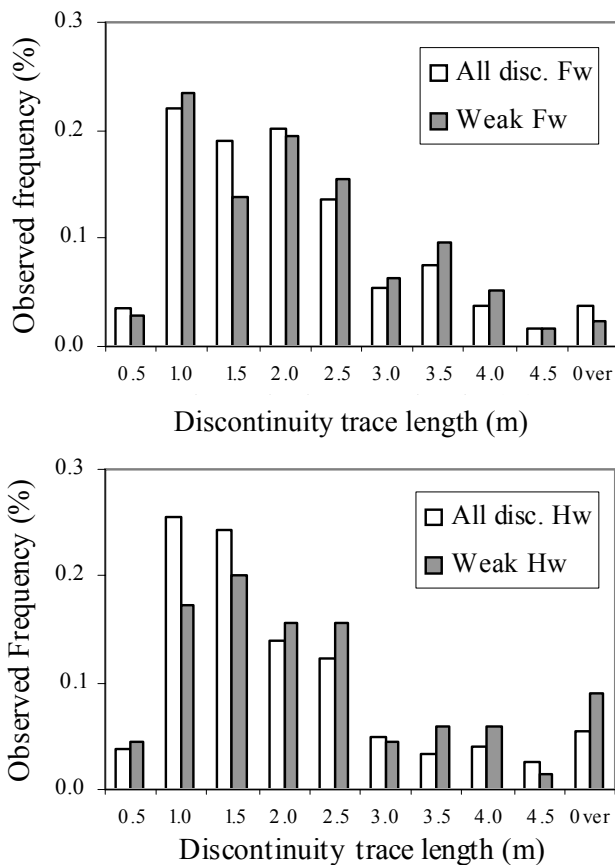| Family set	Data	Thickness distribution observed (%)					
		<1 mm	1 to <2 mm	2 to <3 mm	3 to <5 mm	5 to <10 mm	≥10 mm
Set 1 (subvertical E–W)	53	13.2	35.8	24.5	13.2	9.5	3.8
Set 2 (subvertical N–S)	46	4.3	65.2	17.4	8.8	—	4.3
Set 3 (subhorizontal)	33	6.1	39.4	24.2	21.2	6.1	3.0
Total and mean	136	9.6	46.3	22.1	13.2	5.0	3.7

Figure 12.—Discontinuity trace length from data collected in line mapping.

Therefore, the observed persistence distributions of the discontinuities irrespective of their infill features can be considered to have an isotropic characteristic within the rock mass.

Weak Discontinuity Thickness

Data analysis of the weak vein thickness distribution also showed that no differences between discontinuity sets from the same mapping scale at any sector could be observed. For example, Table 12 shows almost the same weak vein thickness distribution for each set of the data plotted in Figure 5b, which do not differ from when all discontinuities are considered (Tables 8–9). Therefore, the observed thickness distributions can also be considered to have an isotropic characteristic within the rock mass.

Block Size

The weak discontinuity data set from oriented drill core logging was used to stochastically simulate the rock structure and to determine in situ block size distributions [Thompson 2002]. The results are presented in Figure 13. The figure clearly shows that when the strength of the discontinuities is taken into account, the andesite rock type from the Hw sector has a coarser in situ rock block size distribution than the Fw sector. These predicted differences shown in Figure 13 are in accordance with the actual observations at the mine site. However, these differences could not be established by applying rock mass classification schemes (see Table 1).
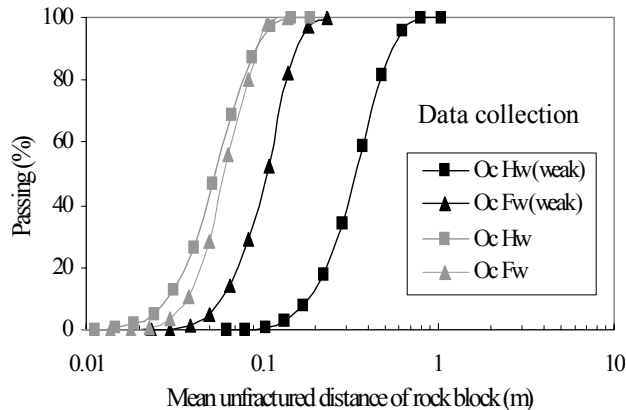
34

Figure 13.—In situ block size distributions from rock structure simulation for weak discontinuities using oriented drill core logging (Oc). Light gray data are from Figure 8.

DISCUSSION

Since conventional rock mass classification systems parameterized mainly open joints to assess rock mass quality [Barton et al. 1974; Hoek et al. 1995; Laubscher 1993], these schemes cannot be readily applied to the rock masses of the primary copper ore at the El Teniente Mine. Even the last upgrade of the Mining Rock Mass Rating (MRMR) [Laubscher and Jakubec 2000] cannot be applied because it does not take into account the multiple mineral ensembles of the vein infill.

Moreover, other discontinuity characteristics that are not clearly included in the classification schemes seem to play a relevant role during rock mass behavior. This is the case for discontinuity thicknesses, which have been found to control rock mass disassembly during caving and the fragmentation process [Brzovic et al. 2006; Brzovic and Villaescusa 2007].

In addition, the discontinuity trace length plays a relevant role in rock mass characterization when a truncation bias length during data collection is adopted. This characteristic must be taken into account if comparisons between different mines are made.

The discontinuity features that have been found to be variable between mine sectors at the El Teniente Mine are the occurrence of veins and their infill characteristic. These particular geological characteristics combined with the in situ rock block distribution seem to be enough to characterize the rock masses of the primary copper ore.

CONCLUDING REMARKS

A data collection campaign designed to characterize the rock structure of the primary copper ore was recently implemented at the El Teniente Mine in central Chile. The results indicated that mainly faults and veins are present within the rock mass. Subvertical faults were defined as

widely spaced, while veins were present in high frequencies in at least three semiorthogonal orientations. Almost no joints were found within the rock mass. Moreover, negligible differences were observed in terms of in situ rock block distributions between the two studied sectors.

A definition of weak discontinuities has been adopted [Brzovic et al. 2006; Brzovic and Villaescusa 2007], which is based on the analysis of rock mass behavior during caving. Only when weak discontinuities are used, the rock mass characterization predicts differences between the two studied sectors. These differences, which are represented in terms of discontinuity frequency and in situ rock block distributions, are in accordance with actual observations at the mine site.

Truncation biases applied during data collection strongly affected the discontinuity set parameters, such as spacing and distribution of thicknesses, and in situ block size distribution. Some discontinuity parameters such as trace length and thicknesses have been found to have an isotropic characteristic within the rock mass. The discontinuity infill has also been found to have an isotropic characteristic, but only within each location, because it changes between sectors. It has also been found that longer discontinuities are statistically thicker than shorter ones, and the infill compositions do not change with their thicknesses. Most of these discontinuity characteristics were found for both weak and all discontinuities.

In conclusion, due to the geological features of the primary copper ore, rock mass classification schemes cannot be readily applied to characterize rock masses at the El Teniente Mine.

REFERENCES

Barton N, Lien R, Lunde J [1974]. Engineering classification of rock masses for the design of tunnel support. Rock Mech *6*(4):189–236.

Brady BGH, Brown TE [2003]. Rock mechanics for underground mining. 3rd ed. London: Kluwer Academics Publisher.

Brooks BA, Allmendinger R, Garrido I. [1996]. Fault spacing in the El Teniente mine, central Chile: evidence for nonfractal fault geometry. J Geophys Res *101*(B6): 13633–13653.

Brzovic A [2001]. Fundamentos geológicos para un sistema de clasificación geotécnico del macizo rocoso

primario, mina El Teniente (in Spanish). Internal report SGL–187/2001 of the Superintendence Geology, CODELCO-Chile, El Teniente Division.

Brzovic A [2005]. Characterization of the primary copper ore for caving at the El Teniente mine, Chile [Draft Dissertation]. Western Australian School of Mines.

Brzovic A, Villaescusa E [2007]. Rock mass characterization and assessment of block-forming geological discontinuities during caving of primary copper ore at the El Teniente mine, Chile. Int J Rock Mech Min Sci *44*(4): 565–583.

Brzovic A, Villaescusa E, Figueroa C [2006]. Characterization of block-forming geological discontinuities during primary ore caving at El Teniente mine, Chile. In: Yale DP, Holtz SC, Breeds C, Ozbay U, eds. Proceedings of the 41st U.S. Rock Mechanics Symposium (Golden, CO, June 17–21, 2006). Alexandria, VA: American Rock Mechanics Association, paper 980.

Cannell J, Cooke D, Walshe JL, Stein H [2005]. Geology, mineralization, alteration, and structural evolution of the El Teniente porphyry Cu-Mo deposit. Econ Geol *100*: 979–1005.

Celhay F, Pereira J, Burgos AL [2005]. Geologia y recursos para el nuevo nivel mina: etapa ingenieria conceptual (in Spanish). Internal report SGL–I–030/2005 of the Superintendence Geology, CODELCO-Chile, El Teniente Division.

Cladouhos T, Marrett R [1996]. Are fault growth and linkage models consistent with power-law distributions of fault lengths? J Struct Geol *18*(2/3):281–293.

Cuadra P [1986]. Geocronologia K-Ar del yacimiento El Teniente y areas adyacentes (in Spanish). Revista Geologica de Chile *27*:3–26.

Garrido I, Riveros M, Cladouhos T, Espineira D, Allmendinger R [1994]. Modelo geologico estructural yacimiento El Teniente (in Spanish). In: Proceedings of VII Congreso Geologico Chileno *2*:1533–1558.

Gillespie PA, Howard CB, Walsh JJ, Watterson J [1993]. Measurement and characteristic of spatial distribution of fractures. Tectonophysics *226*:113–141.

Hobbs BE [1993]. The significance of structural geology in rock mechanics. In: Hudson J, ed. Comprehensive rock engineering. Vol. 1. Pergamon Press, pp. 25–62.

Hoek E, Kaiser PK, Dawden WF [1995]. Support of underground excavations in hard rock. Rotterdam, Netherlands: Balkema.

Hudson JA, Priest SD [1983]. Discontinuity frequency in rock masses. Int J Rock Mech Min Sci Geomech Abstr *20*(2):73–89.

Hurlbut C [1941]. Dana's manual of mineralogy. 15th ed. John Wiley & Sons.

ISRM [1978]. Commission on standardization of laboratory and field test. Suggested methods for the quantitative description of discontinuities in rock masses. Int J Rock Mech Min Sci Geomech Abstr *15*:319–368.

Laubscher D [1993]. Planning mass mining operations. In: Hudson J, ed. Comprehensive rock engineering. Vol. 2. Pergamon Press, pp. 547–583.

Laubscher D, Jakubec J [2000]. The MRMR rock mass classification system for jointed rock masses. In: Hustrulid WA, Bullock R, eds. Underground mining methods: engineering fundamental and international case studies. Littleton, CO: Society for Mining, Metallurgy, and Exploration, Inc.

Rojas E, Cavieres P, Dunlop R, Gaete S [2000a]. Control of induced seismicity at the El Teniente mine, Codelco Chile. In: Chitombo G, ed. Proceedings of MassMin 2000 (Brisbane, Queensland, Australia, October 29–November 2, 2000). Australasian Institute of Mining and Metallurgy (AusIMM), pp. 775–781.

Rojas E, Molina R, Cavieres P [2000b]. Preundercut caving in El Teniente Mine, Chile. In: Hustrulid WA, Bullock R, eds. Underground mining methods: engineering fundamental and international case studies. Littleton, CO: Society for Mining, Metallurgy, and Exploration, Inc., pp. 417–423.

Scholz CH [2002]. The mechanics of earthquakes and faulting. 2nd ed. Cambridge, U.K.: Cambridge University Press.

Skewes MA, Arevalo A, Floody R, Zuniga P, Stern CR [2006]. The El Teniente megabreccia deposit: the world's largest deposit. In: Porter TM, ed. Super porphyry copper and gold deposits: a global perspective. Linden Park, South Australia: PGC Publishing.

Terzaghi K [1946]. Theoretical soil mechanics. John Wiley & Sons.

Thompson AG [2002]. Stability assessment and reinforcement of block assemblies near underground excavations. In: Hammah R, Bawden W, Curran J, Telesnicki M, eds. Proceedings of the NARMS–TAC Conference (July 7–10, 2002). Vol. 2. Toronto, Ontario, Canada: University of Toronto Press, pp. 1439–1446.

Vermilye J, Scholz CH [1995]. Relation between vein length and aperture. J Struct Geol *17*(3):423–434.

Villaescusa E [1990]. A three-dimensional model of rock jointing [Dissertation]. Brisbane, Australia: University of Queensland.

Warburton PM [1980]. A stereological interpretation of joint trace data. Int J Rock Mech Min Sci Geomech Abstr *17*(4):181–190.

Willoner A [2000]. Characterization of rock mass quality and prediction of mass behaviour: an investigation into the parameters which influence the strength of healed joints in hypogene mineralized andesite at El Teniente copper mine, Chile [Thesis]. Leeds, U.K.: University of Leeds, School of Earth Sciences.